Hydrobiologia
DOI 10.1007/s10750-011-0907-x

PRIMARY RESEARCH PAPER

Spatial oxygen heterogeneity in a *Hediste diversicolor* irrigated burrow

Laura Pischedda · Philippe Cuny · José Luis Esteves · Jean-Christophe Poggiale · Franck Gilbert

Received: 18 May 2011 / Revised: 12 September 2011 / Accepted: 25 September 2011

Abstract The heterogeneity of oxygen distribution in a *Hediste diversicolor* burrow environment was investigated in a laboratory experiment using a 6-mm thick tank equipped with oxygen planar optodes. The two-dimensional oxygen distribution in a complete burrow was monitored every 2 min for 4 h. Oxygen concentrations fluctuated over a scale of minutes in the burrow lumen and wall (up to 2 mm) reflecting the balance between worm ventilation activity and oxygen consumption. The magnitude of the three surrounding micro-horizons (oxic, oscillating and anoxic) induced by the intermittent worm ventilation was spatially and temporally variable within the structure. Oxygen variations appeared to be controlled by distance from the sediment–water interface and the direction of water circulation. Moreover, there was an apparent 'buffer effect', induced by the proximity to the overlying water, which reduced the variations of lumen and wall oxygen in the upper part of the structure. These results highlight the heterogeneous distribution and dynamics of oxygen associated with *H. diversicolor* burrows and ventilation activity. They also highlight the necessity of integrating this complexity into the current burrow-base models in order to estimate the ecological importance of burrowing species in coastal ecosystems.

Keywords Bioturbation · Bio-irrigation · Oxygen heterogeneity · *Hediste diversicolor* burrow · Marine sediments

Handling editor: Pierluigi Viaroli

L. Pischedda · P. Cuny · J.-C. Poggiale
Laboratoire de Microbiologie, Géochimie et Ecologie Marines (UMR CNRS 6117), Centre d'Océanologie de Marseille, Université de la Méditerranée, Campus de Luminy, Case 901, 13288 Marseille Cedex 9, France
e-mail: philippe.cuny@univmed.fr

J.-C. Poggiale
e-mail: jean-christophe.poggiale@univmed.fr

J. L. Esteves
Centro Nacional Patagónico, Unidad de Investigación de Oceanografía y Meteorología, Laboratorio de Oceanografía Química y Contaminación de Aguas, CONICET, Bv. Brown 2825, U9120ACF Puerto Madryn, Argentina
e-mail: esteves@cenpat.edu.ar

F. Gilbert (✉)
EcoLab, Laboratoire d'Ecologie Fonctionnelle et Environnement, UPS, INP, Université de Toulouse, 118 route de Narbonne, 31062 Toulouse Cedex 9, France
e-mail: franck.gilbert@univ-tlse3.fr

F. Gilbert
EcoLab,CNRS, 31055 Toulouse, France

Introduction

Macrobenthic fauna profoundly alter the distribution of sediment particles, solutes and microbial communities, especially in coastal marine ecosystems where benthic organisms are densely distributed (e.g. François et al., 2002; Meile & Van Cappellen, 2003;

Published online: 15 October 2011

Papaspyrou et al., 2006; Gilbert et al., 2007). Through sediment reworking and irrigation, a process referred to as bioturbation (*sensu* Richter, 1952), the macrofauna directly affect the decomposition, remineralisation and preservation of organic matter in sediments (Aller, 1994; Reise, 2002). In particular, the gallery-diffusor organisms burrow into otherwise anoxic sediments and actively ventilate them for respiration or feeding purposes (e.g. Anderson & Meadows, 1978; Osovitz & Julian, 2002). The sediment–water interface is increased by their burrowing activity, and in addition worm ventilation activity greatly enhances solute exchanges between the sediments and the overlying water (Fenchel, 1996; Aller, 2001; Pischedda et al., 2008).

Macrofaunal burrows have been extensively studied in terms of sediment reworking (e.g. Duport et al., 2006), morphology (e.g. Davey, 1994), irrigation rate (e.g. Kristensen, 2000), solute distribution and fluxes (e.g. Kristensen & Hansen, 1999), redox oscillations (e.g. Sun et al., 2002), mineralisation rate (e.g. Aller, 1994) and associated microbial communities (e.g. Papaspyrou et al., 2006). However, the distribution and dynamics of solutes within a macrofaunal burrow structure have proven difficult to determine. Consequently, methods such as determinations of global exchanges between the entrance and the exit of the burrow, or local concentration measurements using microelectrode(s) at the burrow openings or localised within or in the vicinity of the burrow structure (e.g. in the burrow wall) have been developed, often in association with simultaneous active ventilation recording (e.g. Kristensen, 1989; Forster & Graf, 1995). Based on these data, efforts have been made to model the solute distribution in actively ventilated burrow environments. Currently, there are two main types of bio-irrigation models: the diffusive tube-irrigation model (Aller, 1980), which was further improved by authors such as Boudreau & Marinelli (1994), Furukawa (2001) and Koretsky et al. (2002), and the advective pocket-injection model (Meysman et al., 2006). One significant difference between these models is that the former is relevant to muddy sediments where bio-irrigation is intrinsically driven by diffusion across the burrow wall, whereas the latter describes sandy sediments where active ventilation by worms induces the advective transport of water in the surrounding sediments due to the higher permeability of sands (Foster-Smith, 1978).

Due to the lack of data about solute distribution, these bio-irrigation models do not include the macro- and micro-scale heterogeneity of solute distribution within the burrow and in its immediate vicinity. The introduction of planar optodes into benthic ecology now makes it possible to determine the 2D distribution and dynamics of oxygen, ammonium, pCO_2 or pH in sediments (e.g. Glud et al., 1996; Hulth et al., 2002; Stromberg & Hulth, 2003; Zhu et al., 2006). With regard to oxygen, so far only a few studies have been undertaken using planar optodes to monitor oxygen distribution and dynamics in macrofaunal burrows. For instance, Timmermann et al. (2006), Polerecky et al. (2006) and Behrens et al. (2007) reported a highly dynamic pattern of oxygen distribution in laboratory experiments with the polychaete *Arenicola marina*, the sand eel *Ammodytes tobianus* and the Chironomid larvae *Chironomus plumosus*, respectively. In shallow water environments, Wenzhöfer & Glud, (2004) reported patchiness and variability of the benthic oxygen distribution on a diel scale, primarily induced by the distinct diel pattern in *Hediste diversicolor* activity and photosynthesis. More precisely, they showed that the volume of oxic sediments around burrow structures was influenced by these changing environmental conditions, and that oxygen uptake through the burrow walls just after sunset accounted for most of the total oxygen uptake. In those studies, however, the oxygen distribution and dynamics were only quantified in particular or localised areas of the burrows, and this did not make it possible to define the oxygen heterogeneity in a complete bio-irrigated burrow.

Hediste diversicolor (OF Müller, 1776) is a polychaete worm widely distributed in estuarine and lagoonal habitats from North Africa to North Europe (Mettam, 1979; Gillet, 1993) at a density of 500–5,000 individuals per square metre (Vedel & Riisgard, 1993). This species shows high physiological tolerance of extreme variations in environmental factors, and can grow and reproduce in different sediment types and also in stressed environments (e.g. Bartels-Hardege & Zeeck, 1990; Miron & Kristensen, 1993; Scaps, 2002). It lives in a semi-permanent U- or Y-shaped mucus-lined burrow extending 6–12 cm into muddy or sandy–muddy sediments. The worm actively ventilates its burrow structure (Kristensen, 1981; Davey, 1994) with regular alternations of active ventilation periods of $\sim$10 min followed by rest periods of $\sim$5 min (Kristensen, 2001).

The aim of the present laboratory study involving planar optodes was to determine the heterogeneous 2D

oxygen distribution and dynamics in different areas of an entire *H. diversicolor* burrow structure, and to compare the associated oxygen penetration depth and diffusive fluxes at the surface and across the burrow sediment–water interfaces.

Materials and methods

Experimental setup

The *H. diversicolor* specimens used in this study (8.9 ± 2.1 cm long; mean ± SD; $N = 19$) and the sandy-mud sediments were collected in September in the Carteau cove (Gulf of Fos, Mediterranean Sea) by shovel sampling in the Saint-Antoine canal at a depth of 0–0.5 m (43°22′30.40″N/4°50′20.80″E). In the laboratory, the worms were placed in tanks filled with the experimental sediment and aerated overlying seawater (38 ± 0.2 psu). They were acclimatised to the experimental conditions (water temp.: 24 ± 1°C, natural photoperiod) for 2 weeks before the start of the experiment.

Two and a half weeks before the beginning of the experiment, the four transparent sides of a polycarbonate tank (20 × 20 × 20 cm) were fitted with square oxygen optodes which had been previously cut (19 × 19 cm) to fit inside the tank. A PVC cube was then inserted into the tank in order to reduce the sediment thickness to 6 mm in front of each optode and make the worms and their galleries visible. The tank was then filled with a depth of about 11 cm of sieved sediments and 6–8 cm of aerated overlying water (24 ± 1°C, 38 ± 0.2 psu). Five days later, oxygen measurements constituting the control values were performed, then the organisms ($N = 19$) were placed in the tank (T_0). They immediately started to explore their environment and construct their burrows. In order to avoid the development of a microbial biofilm on the optode, especially within the burrows that are a highly favourable microenvironment for microbial activity, oxygen measurements were done 3 days after the introduction of the worms on the side of the tank where most of a burrow was visible (Fig. 1). Measurements were performed every 2 min for 4 h, and provided a time series of 121 oxygen images associated with the 121 sediment structure images used to detect the sediment–water interface.

Image acquisition

The two-dimensional oxygen concentration in bioturbated sediments and the overlying water was quantified with semi-transparent planar oxygen optodes. Oxygen measurement was based on the dynamic quenching of oxygen on an immobilised fluorophore (Kautsky, 1939). The optical sensor was composed of two thin layers, a transparent polyester support foil (HP transparency, C2936A, ∼150 µm thick) and a sensing layer, in which the platinum (II) mesotetra (pentafluorophenyl) porphyrin oxygen-quenchable fluorophore (Pt-PFPP, Frontier Scientific Inc.) was embedded in a polystyrene matrix (∼20 µm) (Papkovsky et al., 1992; Liebsch et al., 2000). The sensing layer mixture was composed of 3 mg of Pt-PFPP dissolved in 3 ml of toluene (Rathburn Chemicals Ltd, Acros Organics) and 0.65 g (5%) of polystyrene pellets (Acros Organics) dissolved in 15 ml of toluene. The two solutions were mixed and spread on the polyester support foil (300 cm^2). The solvent was left to evaporate slowly until the membrane was completely dry.

Oxygen optodes were calibrated by a three-point calibration method. For the two intermediate calibration points (90%, air bubbling and 50%, N_2 bubbling), the oxygen concentration was first measured just behind the optode using an oxygen probe (LDO HQ10, Hach), immediately followed by capture of the oxygen image. In order to avoid problems due to uneven illumination or dye distribution (Strömberg, 2006), the 0% saturation reading was taken in anoxic sediment close to the zone studied, i.e. at the sediment surface (S) or in the overlying water (OW), and in five zones of the *H. diversicolor* burrow corresponding to the inhalant opening zone (A1), two intermediate zones at mid-depth (A2 and A4), the bottom zone (A3) and the exhalant opening zone (A5), respectively (Fig. 1a). No further calibration was performed in the water environment after the experiment had begun, because it was difficult to remove sediments without damaging the optodes. However, data were corrected for drift, which was quantified on the basis of the change in the oxygen level over time in the anoxic sediment close to each of the zones studied.

The optical system combined with the use of the oxygen optode made it possible to take high resolution images of sediments and to measure the corresponding

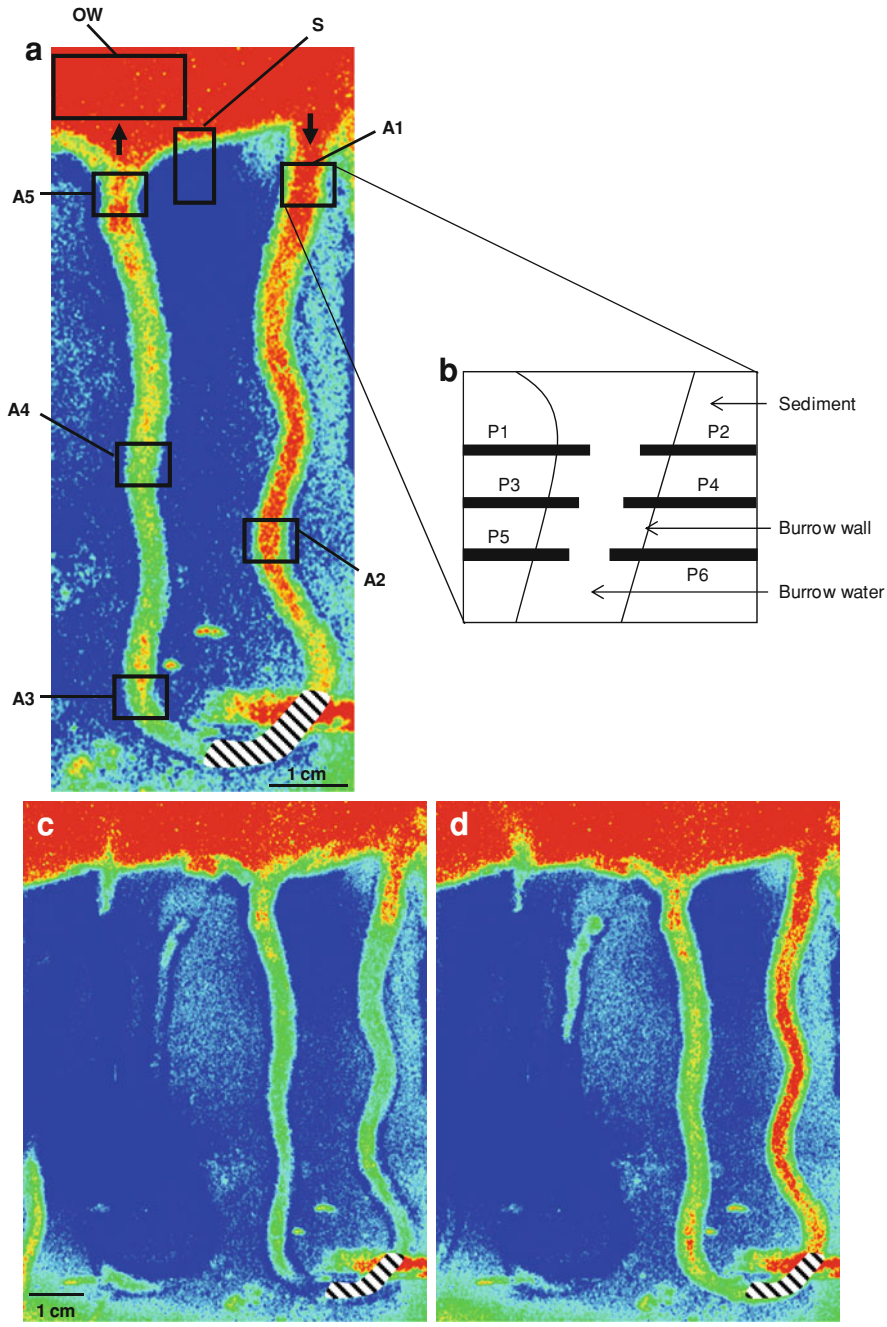

Fig. 1 (Colour online) **a** Optode image (*grey scale* images converted to false colour) of oxygen distribution in sediments and in an *H. diversicolor* burrow and location of the zones investigated during the study (burrow zones: A1–A5; surface: S; overlying water: OW). Hatched zone: part of the burrow lumen that could not be observed because it was occupied by the worm; *arrows* direction of water flow during ventilation. **b** Example of areas (P1–P6) selected for the extraction of oxygen profiles for diffusive oxygen flux calculation. **c**, **d** examples of full recorded optode images of oxygen distribution in periods of low and high water oxygen concentration in the burrow, respectively

oxygen concentration. For full details of the experimental set-up, see Pischedda et al. (2008). In brief, the optode was excited by a Xenon lamp light (Perkin Elmer, 300 Watts) passing through a shutter and an excitation glass filter (405 ± 10 nm, Omega Optical) mounted on a first filter wheel. Light emitted by the optode sensing membrane was collected through a Nikon macro lens and an emission glass filter (654 ± 24 nm) mounted on a second filter wheel. The fluorescence signal was then detected by a Peltier-cooled 12-bit monochrome CCD camera (KAI 2000, 1,600 × 1,200 pixels, 7.4 × 7.4 µm). Images were taken in darkness with an integration time of 30 s for oxygen and of 1 s for the sediment structure (without

any filter). The light shutter, excitation and emission filter wheels and camera were computer-controlled using the Image Pro Plus—Scope Pro package installed on a Pentium 4 computer. The digital TIFF images were then stored using 12-bit grey scale (0–4,095). The acquisition and storage of oxygen images were automated with a custom-made script.

Image processing

A non-linear relationship slightly modified from the Stern–Volmer equation (Klimant et al., 1995) was used to convert the pixel intensity (arbitrary units) into oxygen concentration as follows:

$$I = I_0[\alpha + (1-\alpha)(1/1 + K_{sv}C))]$$

where I_0 is the fluorescence intensity in the absence of oxygen, C is the oxygen concentration (µmol/l), K_{sv} is the quenching constant expressing the quenching efficiency (M^{-1}) and α is the non-quenchable fraction of the luminescence including scattered stray light. The constants α and K_{sv} were determined from I_0 and the two intermediate calibration points, with oxygen concentrations C_1 and C_2 corresponding to intensities I_1 and I_2, respectively, and integrated into the following equations:

$$K_{sv} = [I_0(C_2 - C_1) - (I_1C_2 - I_2C_1)]/[(I_1 - I_2)C_1C_2]$$

$$\alpha = [I_1(1 + K_{sv}C_1) - I_0]/(I_0K_{sv}C_1)$$

α and $K_{sv,}$ were averaged for each zone studied taking into account the closest anoxic zone. Having estimated α, K_{sv} and I_0, the oxygen concentration was obtained by rearranging the first equation:

$$C = (I_0 - I)/(K_{sv}(I - I_0\alpha)$$

Due to the problems we have already mentioned, the oxygen optode was calibrated specifically for each zone studied. Table 1 shows the variation in the constants K_{sv} and α calculated from data extracted within a 50 × 50 pixel area. K_{sv} ranged from 20.6 ± 2.6 × 10^{-3} M^{-1} (A3, mean ± SD, N = 2,500) to 26.8 ± 2.9 × 10^{-3} M^{-1} (A5, mean ± SD, N = 2,500), which corresponded to a maximum of 13% variation from the mean value, 23.7 ± 2.4 × 10^{-3} M^{-1} (mean ± SD, N = 2,500). The variation in K_{sv} induced a variation in α of 0.7% around the mean value, 77.1 ± 0.4 × 10^{-2} (mean ± SD, N = 2,500). Based on the mean constants, the oxygen value corresponding to an intensity of 88.6 (arbitrary unit) was 190.5 µmol l^{-1}, which may have varied by up to 2.3% depending on the zone considered, with a global calibration. This confirms that the differences in the K_{sv} values did indeed have a significant effect on oxygen concentration values, but this was limited by the separate calibration of the oxygen optode for each of the zones studied.

Vertical oxygen profiles extracted from 2D oxygen measurements were used to determine diffusive oxygen fluxes ($J_{(z)}$, mmol m^{-2} d^{-1}), which were calculated from Fick's first law of diffusion, based on the assumption that molecular diffusion was the main oxygen transport mechanism involved (Berner, 1980; Jørgensen & Revsbech, 1985; Rasmussen & Jørgensen, 1992):

$$J_{(z)} = -\Phi D_s \partial C_{(z)}/\partial_z$$

where Φ is the porosity (0.69), C is the oxygen concentration (µmol l^{-1}), z is the depth of oxygen penetration into sediments (cm) and $\partial C_{(z)}/\partial z$ is the oxygen gradient. D_s is the oxygen diffusion coefficient in sediments (1.24 × 10^{-5} cm^2 s^{-1}), which was calculated on the basis of the following relationship (Berner, 1980): $D_s = D_0/\theta^2$, where θ is the tortuosity and D_0 is the diffusion coefficient of oxygen in water (cm^2 d^{-1}). Finally θ^2 may be estimated from the following equation (Boudreau, 1996): $\theta^2 = 1 - \ln(\Phi^2)$.

Because the data set was composed of numerous images (N = 121, image size: 9.3 × 3.7 cm, pixel size: 800 × 800 µm), they were processed using MatLab® software, which applied the required procedure successively to the 121 images. A low-pass filter (3 × 3 pixels) was applied to the raw images and the pixel fluorescence intensity was converted into oxygen concentration. The MatLab® script made it possible to extract the oxygen concentration in each of the zones studied (Fig. 1a). Oxygen concentration was averaged for each zone in the 121 images. In order to measure the oxygen penetration and calculate the oxygen diffusive flux, three oxygen profiles at the sediment surface and six profiles in each burrow zone were extracted (P1, P2 and P3 on the left side of the burrow wall, and P4, P5 and P6 on the right side, Fig. 1b). Each extracted profile corresponded to six neighbouring pixel lines, which were averaged. The sediment–water interface at the surface and in the burrow was located manually on corresponding

Table 1 Coefficients K_{sv} and α calculated from data extracted within a 50 × 50 pixels area ($N = 2{,}500$), for each zone of the *H. diversicolor* burrow studied (surface and A1–A5)

Zone	K_{sv} (10^{-3} M^{-1})		α (10^{-2})		O_2
	Mean	SD	Mean	SD	μmol/l
Surface	26.9	3	77.7	0.4	194.1
A1	22.7	3.5	76.9	0.6	188.0
A2	22.1	2.2	76.9	0.4	193.1
A3	20.6	2.6	76.6	0.6	193.9
A4	22.9	2.3	77	0.4	190.8
A5	26.8	2.9	77.7	0.4	194.8
Mean value (±SD)	23.7 ± 2.4		77.1 ± 0.4		190.5

greyscale images. Another custom-made MatLab® script allowed the oxygen gradient at the sediment–water interface to be calculated, in order to calculate the diffusive flux. The depth to which oxygen penetrated into the sediment was located automatically and for each oxygen profile, was taken to be the depth where the oxygen value dropped below 1 μmol l^{-1}.

Statistical analyses

Statistical comparisons between time series of oxygen concentration, flux and penetration data in the zones studied were performed with a non-parametric Friedman test (121 observations for each of the 6 samples, i.e. the zones studied). When a significant difference was observed between samples (5% tolerance), a multiple paired comparison was performed following the Nemenyi procedure (bilateral test). Linear regressions between temporal series were performed with the correlation matrix of Pearson (5% tolerance). The time-lag between the time series was determined on the basis of the better linear regression obtained by progressively shifting one temporal series with respect to another. The symmetry between the oxygenation of the right and the left part of the zones studied in the burrows was evaluated by an asymmetry index (S), which was calculated by integrating their differences. The integral was calculated on the basis of the Riemann method, corresponding to the sum of the squared differences between the right and left parts in each zone, multiplied by the interval of the measurement. The result was then divided by 10 to obtain the asymmetry index AS. The greater the value of AS, the more asymmetric the samples.

Results

Visual observations of the burrows

Unfortunately, only one of the *H. diversicolor* specimens constructed a U-shaped burrow (approximately 8 cm deep) that was completely adjacent to a side of the tank and therefore clearly visible. The lumen of this burrow was visible almost in entirety, except for one small area in the bottom part where the worm was located (Fig. 1a). Most of the sediment was greyish-brown, indicating that it was reduced, except for a light-brown layer a few millimetres thick of oxidised sediment along the burrow wall and at the surface. During the experiment, we observed that the worm stayed in the bottom part of the burrow with its head facing towards the right side. The ventilation was unidirectional and water circulated from the worm's head to tail, i.e. water entered from the inhalant opening zone A1 and left the burrow via the exhalant opening zone A5.

Burrow oxygen concentrations

Burrow structures extended the oxic sediment–water interface, allowing oxygen to penetrate deep into the anoxic sedimentary column (Fig. 1c, d). The oxygen concentration in overlying water varied between 126.0 and 146.0 μmol l^{-1}, with a mean of 133.1 ± 3.5 μmol l^{-1} (mean ± SD, $N = 121$, Fig. 2). One should note that these mean oxygen values were low because of the stratification of the tank water column in the absence of water mixing. Oxygen values of around 200 μM were measured (data not shown) in the upper part of the water column where the system was aerated, but the oxygen level decreased as it approached the sediment due to oxygen consumption

by the sediment. The area used to calculate the mean oxygen concentration of the overlying water was principally positioned close to the sediment, and therefore gave low mean values. During the experiment, the oxygen concentration recorded in the burrow lumen varied between 27.4 μmol l^{-1} (A4) and 90.9 μmol l^{-1} (A1), with a mean value of 56.4 ± 15.3 μmol l^{-1} (mean ± SD, $N = 605$, Fig. 2). The mean oxygen concentration of water passing through the burrow varied between 78.0 ± 7.3 μmol l^{-1} (A1, mean ± SD, $N = 605$) and 42.3 ± 8.0 μmol l^{-1} (A4, mean ± SD, $N = 605$). Oxygen concentration decreased from the burrow inhalant opening (A1) to the intermediate zone (A4), and increased slightly at the exhalant opening (A5: 58.0 ± 4.7 μmol l^{-1}, mean ± SD, $N = 605$). It was significantly different in each zone, except for zones A3 and A4 (Fig. 2).

During the experiment, oxygen concentration continuously fluctuated in the burrow lumen (Fig. 3). The amplitude of these fluctuations was most pronounced in the intermediate and bottom zones A2 and A3, respectively (Fig. 2). The change in oxygen concentration over time in neighbouring zones, such as A2 and A3 (linear regression, $R^2 = 0.38$) or A3 and A4 ($R^2 = 0.36$), was small compared with that between more distant zones such as A1 and A4 ($R^2 = 0.05$) or A2 and A4 ($R^2 = 0.02$).

Oxygenation of the burrow wall

During the experiment, the distance to which oxygen penetrated into the sediment ranged from 1.67 to 3.27 mm at the surface, with a mean value of 2.57 ± 0.24 mm (mean ± SD, $N = 363$), and from 0.48 to 3.27 mm in the burrow wall, with the mean value varying in the different zones (Fig. 4). Oxygen penetrated least deeply in zones A2 (1.91 ± 0.46 mm, mean ± SD, $N = 726$) and A3 (1.82 ± 0.67 mm, mean ± SD, $N = 726$), whereas it penetrated most deeply in zone A1 (2.62 ± 0.29 mm, mean ± SD, $N = 726$). Each zone had an oxygen penetration distance that differed significantly from that of the other zones, except zones A4 and A5 (Fig. 4).

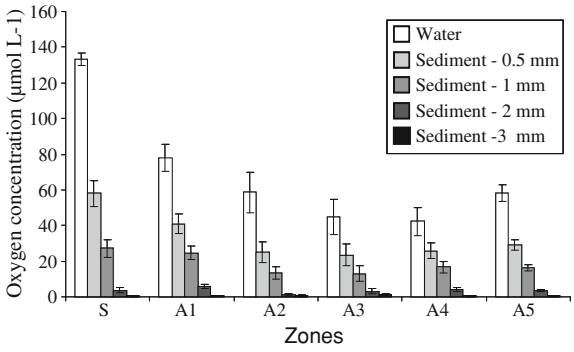

Fig. 2 Mean oxygen concentrations in free water and sediments (0.5–3 mm distance from the interface) into the overlying water and the *H. diversicolor* burrow (OW and zones A1–A5, respectively). *Error bars* represent the standard deviation (SD) for $N = 121$

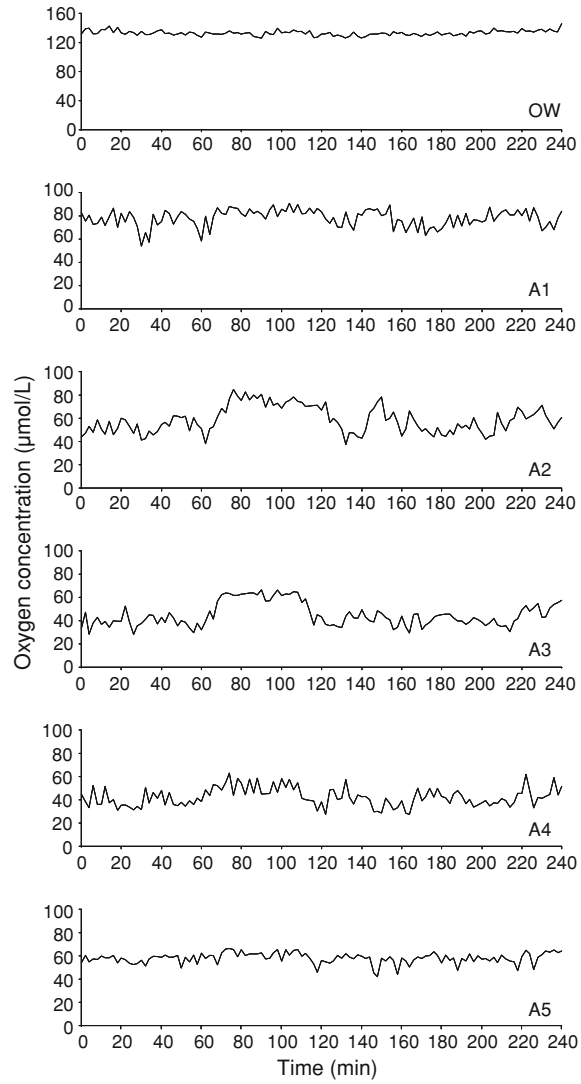

Fig. 3 Dynamics of the oxygen concentration in overlying water (OW) and in the *H. diversicolor* burrow lumen (zones A1–A5) during the experiment

Within the burrow wall, oxygen concentration was monitored up to 3 mm from the lumen. For each zone, the mean oxygen concentration decreased with increasing distance from the lumen (Fig. 2). The wall oxygen concentration was 43–61, 23–40, 1–7 and <2% of the lumen concentration at 0.5, 1, 2 and 3 mm distances from the lumen, respectively. Despite these lower concentrations, the oxygen dynamics presented a similar pattern to those in the lumen, at least as far as 1 mm into the wall, with oxygen concentration decreasing from the inhalant opening towards the bottom, and then slightly increasing up to the exhalant opening A5 (Fig. 2). From a temporal point of view, as illustrated for the bottom zone of the burrow (A3, Fig. 5), oxygen fluctuations were also detected within the wall, but with lower amplitudes. The best linear correlations were obtained with a time-lag of zero ($R^2 = 0.91$), 2 ($R^2 = 0.82$) and 6 min ($R^2 = 0.72$) at 0.5, 1 and 2 mm, respectively.

Looking more precisely at oxygen penetration into the burrow wall, and more especially at the duration of oxygenation (i.e. the time during which some oxygen is present as a percentage of the total duration of the experiment) in the first few millimetres of the right and left parts of the burrow, a radial dissymmetry based on the oxygenation level was detected in each zone (Fig. 6). The bottom zone (A3) and the exhalant opening zone (A5) appeared to display the greatest asymmetry (i.e. the greatest difference between the left and right parts of the burrow), estimated by asymmetry indices, AS, of 315 and 333, respectively. Zones A2 (AS = 56) and A4 (AS = 48) presented intermediate asymmetries, and the inhalant opening zone (A1) was the most symmetrical (AS = 3).

The area of oxygenated sediments observable on the oxygen images was on average 8.4 ± 0.8 cm^2 (mean ± SD, $N = 121$), 87% of which was due to the presence of the burrow. Moreover, if we consider the burrow itself, the mean surface of oxygenated sediment was 7.3 ± 0.8 cm^2 (mean ± SD, $N = 121$); this was 20% higher during the active periods of worm ventilation activity and 20% lower during the rest periods.

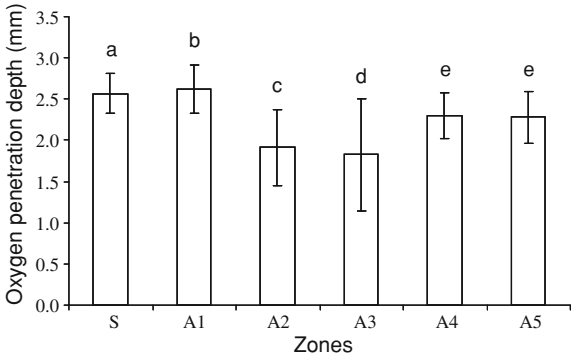

Fig. 4 Mean oxygen penetration depth at the sediment surface and in the wall of the *H. diversicolor* burrow (zones A1–A5). *Error bars* represent the standard deviation (SD) for $N = 363$ (surface) and $n = 726$ (burrow). *Letters a, b, c, d* and *e* correspond to significant differences between the zones studied (non-parametric Friedman test, 5% tolerance significance level, and multiple paired comparisons following the bilateral test, Nemenyi procedure)

Oxygen diffusive flux

The diffusive flux of oxygen at the surface ranged from 1.4 to 12.7 mmol m^{-2} d^{-1}, with a mean of 6.50 ± 1.46 mmol m^{-2} d^{-1} (mean ± SD, $N = 363$), whereas the flux across the burrow wall ranged from 0.7 to 6.6 mmol m^{-2} d^{-1} (Fig. 7). Like the mean oxygen distribution in the burrow lumen, the mean diffusive flux decreased from the inhalant opening zone (A1, 4.07 ± 1.01 mmol m^{-2} d^{-1}, mean ± SD, $N = 726$) towards the intermediate zone A4

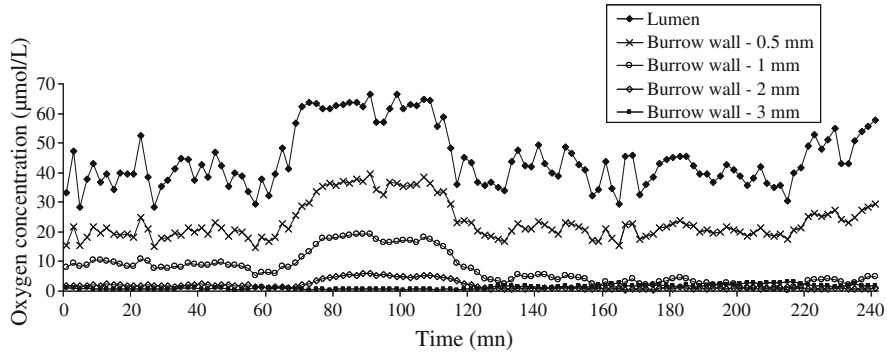

Fig. 5 Oxygen dynamics in the lumen and wall of the *H. diversicolor* burrow (0.5–3 mm distance from the lumen) in the bottom zone A3. Values are the means of the six profiles in each zone

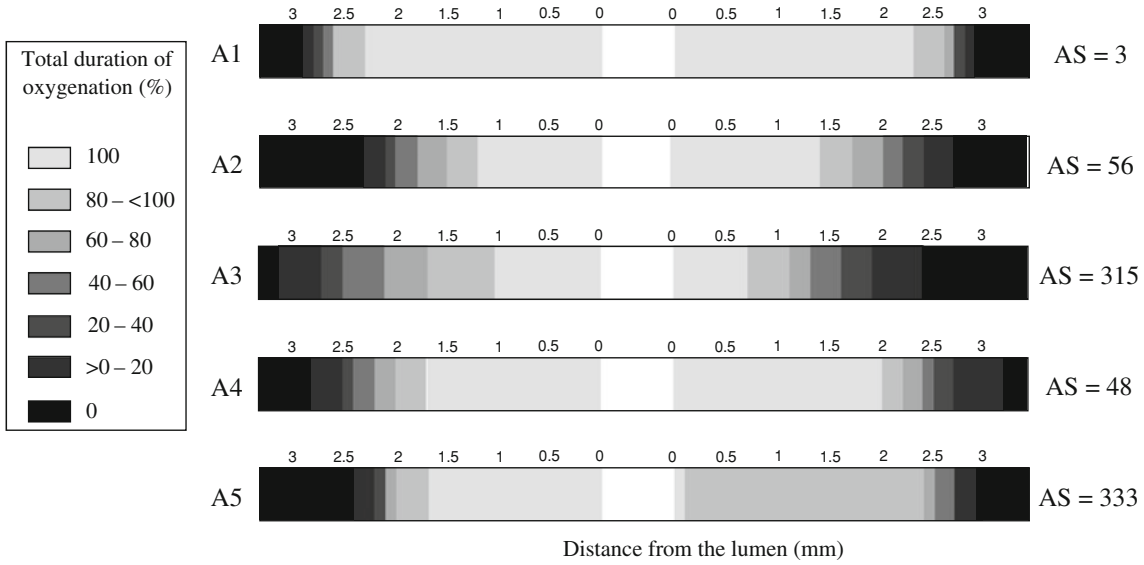

Fig. 6 Duration of oxygenation (i.e. the time during which some oxygen is present as a percentage of the total duration of the experiment) in the first few millimetres of the right and left parts of the burrow, for zones A1–A5. The symmetry between the oxygenation of the right and the left sides is quantified by the asymmetry index (AS) (see text)

(1.92 ± 0.49 mmol m^{-2} d^{-1}, mean ± SD, $N = 726$), and then increased slightly at the exhalant opening (A5, 2.48 ± 0.69 mmol m^{-2} d^{-1}, mean ± SD, $N = 726$). Fluxes exhibited high variability, especially at the surface, in the inhalant opening zone (A1) and in the intermediate zone located immediately beneath it (A2, 3.65 ± 0.80 mmol m^{-2} d^{-1}, mean ± SD, $N = 726$). The oxygen diffusive flux values were all significantly different, except between zones A1 and A2 and between zones A3 and A5 (Fig. 7).

Oxygen penetration and diffusive flux within the burrow wall both exhibited the same temporal pattern as those in the lumen. As illustrated by Fig. 8 for the bottom zone (A3), both varied in accordance with the concentrations of oxygen in the water, with a time-lag of about 4 min for the oxygen penetration depth ($R^2 = 0.47$), and with no time-lag for the diffusive flux ($R^2 = 0.38$).

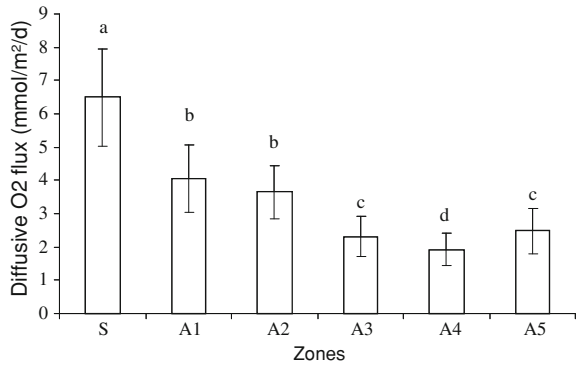

Fig. 7 Mean diffusive oxygen fluxes at the surface and in the *H. diversicolor* burrow (zones A1–A5). *Error bars* represent the standard deviation (SD) for $N = 363$ (surface) and $n = 726$ (burrow). *Letters a, b, c* and *d* correspond to significant differences between the zones studied (non-parametric Friedman test, 5% tolerance significance level, and multiple paired comparison following the bilateral test, Nemenyi procedure)

Discussion

Oxygen fluctuations in the *H. diversicolor* burrow

Previous studies that specifically monitored the macrofaunal ventilation cycle were based on measuring water flow rather than on directly measuring oxygen levels within the burrow (for a review, see Riisgard & Larsen, 2005). Specific studies of *H. diversicolor* have shown that this species intermittently ventilates its burrow following a regular cycle of active (~10 min) and resting phases (~5 min) (e.g. Kristensen, 1981). No clear ventilation pattern was detected in the burrow lumen in this study, mainly because of the method of data acquisition, where each oxygen picture

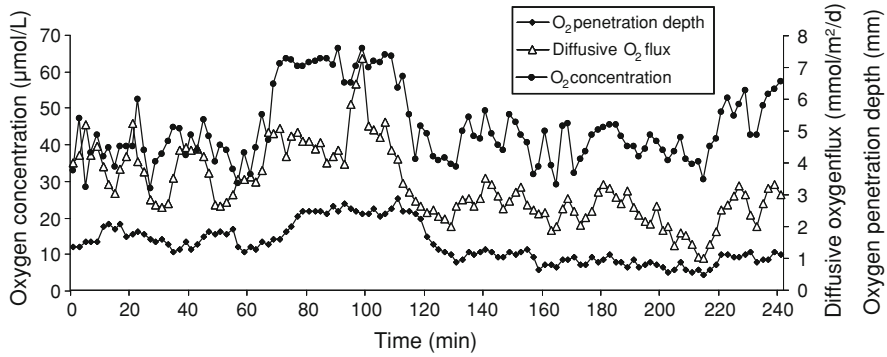

Fig. 8 Dynamics of the oxygen concentration in the lumen, the diffusive oxygen flux and the depth to which oxygen penetrated in the *H. diversicolor* burrow wall, in the bottom zone (A3)

represented an event lasting 30 s, which corresponded to the time required for image acquisition. Moreover, the interval between two measurements was 2 min, which limited our ability to assess the worm ventilation cycle within the burrow. However, our results do show that oxygen concentration fluctuated at a scale of minutes in the burrow, and we can reasonably link this to worm ventilation activity. A similar pattern was detected within the burrow wall, where oxygen concentrations reflected those in the lumen, as previously reported for other ventilating species such as the polychaetes *A. marina* (Timmermann et al., 2006) and *Lanice conchilega,* and the crustacean *Callianassa subterranea* (Forster & Graf, 1995). However, while we observed decreasing amplitudes of oxygen fluctuations in correlation with increasing distance from the lumen, we also observed an increasing time-lag in the oxygen dynamics in the lumen. The latter, which was related to patterns of change in both oxygen penetration depth and diffusive flux, was clearly dependent on the time taken for oxygen to diffuse from the lumen to the wall.

Increases in oxygen concentration and penetration into the burrow wall were closely associated with active macrofaunal ventilation. We were able to distinguish three micro-horizons in the burrow wall, presumably resulting from intermittent worm bio-irrigation: a permanently oxic layer, a layer oscillating between oxic and anoxic conditions and, at a distance too far from the burrow lumen to allow oxygen to penetrate, a permanently anoxic layer ($O_2 < 1$ µmol l^{-1} in this study). The two first layers corresponded to a thickness that was spatially variable within the structure and highly dynamic (±20%) following the worm ventilation pattern. This oxygen zoning is of major importance, since it has been shown that rates and pathways of organic matter degradation are not the same under oxic, anoxic and oscillating redox conditions (Sun et al., 2002). In fact, organic matter degradation can occur up to ten times as fast under oxic as under anoxic conditions (Kristensen, 2000). Furthermore, redox oscillations are accompanied by rapid switches in the dominant bacterial metabolism, influencing both organic matter burial and geochemical cycles (Hansen & Kristensen, 1998; Rosenberg, 2001). For instance, Caradec et al. (2004) found that the continuous or a periodic presence of oxygen stimulated the degradation of some lipids (triacylglycerols) and the subsequent degradation of the metabolites released (e.g. free fatty acids), leading to lower residual concentrations of such lipids in the sediment than under anoxic conditions.

Oxygen spatial heterogeneity

In this study, the burrow exhibited significantly lower oxygen concentrations than the overlying water. The maximum oxygen concentration in the burrow lumen, observed in the most highly oxygenated zone (i.e. the inhalant opening zone A1) was only 70% of the mean oxygen concentration in overlying water (133.1 ± 3.5 µmol l^{-1}). In addition, the composition of the burrow water did not remain identical to that of the overlying water during ventilation. Indeed, the volume of water replaced by each pumping of the macrofauna is smaller than the volume of the burrow cavity, and the velocity of water due to macrofauna flushing has a finite value (Aller et al., 1983; Kristensen et al., 1991). The low concentration of oxygen in the burrow demonstrates that *H. diversicolor* can live without highly oxygenated water, as already suggested by its high ecological tolerance of sulphide (Vismann, 1990). Under unfavourable environmental conditions, such as low oxygen concentration, *H. diversicolor* is able to regulate oxygen uptake by a combination of

behavioural and physiological mechanisms (e.g. an increase in ventilation activity, the optimisation of oxygen extraction; Kristensen, 1983). It is also able to switch to extended anaerobiosis during persistent anoxia or excessive levels of sulphide (Schottler, 1979; Jahn et al., 1992).

The *H. diversicolor* burrow displayed a heterogeneous distribution of oxygen, as shown by the decreasing trend from the inhalant opening down to the burrow bottom, and then a slight increase up to the exhalant opening. This reflects the progressive consumption of oxygen as water circulates within the burrow lumen during active ventilation. In fact, burrow oxygen is consumed by both worm and microbe respiration and by re-oxidation of inorganic metabolites produced by anaerobic metabolisms in surrounding sediments (Jørgensen, 1983). Although the fauna is important for the benthic oxygen uptake, faunal respiration itself constitutes only a minor part of the total fauna-related oxygen consumption, as demonstrated by experimental and in situ measurements (e.g. Kristensen, 1985; Glud et al., 2003; Dunn et al., 2009; Papaspyrou et al., 2010).

The above discussion is based on the assumption that the burrow constitutes a homogeneous structure, which both the inter- and intra-zone (asymmetry) comparisons reported here indicate is clearly not the case. Despite the initial homogenisation of the sedimentary matrix before the experiment, the surrounding sediments, and the burrow wall in particular, may give rise to patchiness. For example, mucous secretions may have been irregularly distributed along the burrow wall, influencing (1) the local intensity of microbial reactions, since the mucus layer is composed of labile organic substances and (2) the local thickness of the layer through which oxygen may diffuse, even if the mucus layer is not considered to be a barrier to oxygen diffusion (Aller, 1988; Fenchel, 1996; Hannides et al., 2005). We also observed that the amplitude of oxygen fluctuations was less pronounced in the upper part of the burrow than in the lower part. This phenomenon is probably due to the proximity of the upper zones (A1 and A5) to the oxygen-rich overlying surface water. Surface dissolved oxygen, which was present in limitless quantities in the overlying water, may have been constantly diffusing into these nearby upper burrow zones, resulting in a 'buffer effect'. Deeper down in the sediments, i.e. further from the oxygen reservoir, the burrow did not benefit from this effect and the amplitude of oxygen fluctuation was therefore greater. The impact of the buffer effect was observed not only in the burrow lumen, but also in the burrow wall, where the radial dissymmetry of oxygenation was higher in the bottom zone.

Influence of oxygen distribution heterogeneity on diffusive flux

Diffusive oxygen flux was calculated on the basis of the profiles extracted from the oxygen images. However, as emphasised by Glud et al. (1996), the wall effect of the tank induces distortion of the diffusive boundary layer (DBL), which makes simple calculations of the diffusive flux based on DBL-based data less meaningful. Nevertheless, we considered that the calculated fluxes could be used as comparative data in this study. Diffusive oxygen fluxes within the burrow wall were on average 1.5–3.5 times lower than those in the surface sediments. In a similar experiment, Pischedda et al. (2008) found equivalent or lower diffusive oxygen fluxes in the *H. diversicolor* burrow compared with surface sediments. The oxygen concentration in the burrow could explain these lower fluxes. Our results showed that diffusive fluxes in the burrow were directly influenced by the oxygen concentration in the lumen, since they followed the same spatial and temporal pattern. For example, when oxygen concentration increased within the lumen, it diffused in a radial pattern towards the burrow wall, generating a steeper gradient at the sediment–water interface and resulting in a higher flux. Therefore, it is reasonable to assume that fluxes in the burrow were lower than those in the surface because of the lower oxygen concentration in the burrow. Moreover, some of the oxygen consumed within the burrows is used for the chemical and biological reoxydation of reduced compounds (e.g. iron (II) and sulphide). Two-dimensional zonations of these reduced compounds have been shown to be highly heterogeneous in bioturbated sediments, particularly in the vicinity of burrows and roots (Robertson et al., 2009; Bertics et al., 2010; Bertics & Ziebis, 2010; Pagès et al., 2011), which could potentially drive variable fluxes of both reduced compounds and oxygen in the different part of the burrows.

Differences between diffusive fluxes at the surface and in the burrow are also likely to be linked to the microbial nature of the sedimentary matrix. The

burrow structure is not simply an extension of the sediment surface, but has unique physical–chemical properties and microbial community characteristics that may indirectly influence oxygen uptake (Aller & Aller, 1986; Papaspyrou et al., 2005). Burrow walls have been shown to be microbial degradation hotspots, presenting different bacterial assemblages and higher bacterial abundance and activity rates than surface sediments (e.g. Marinelli et al., 2002; Papaspyrou et al., 2006). These differences could be linked to the mucus lining, which directly enriches the burrow wall with labile organic matter, but can also act as a trap for phytoplankton (Defretin, 1971; Kristensen, 2000).

A representative and 'typical' burrow?

This study was based on a single *H. diversicolor* burrow. Indeed, only one individual produced a complete structure during the experiment. However, we also looked at another randomly chosen burrow (Fig. 9a), and found that despite its incomplete structure, it displayed similar oxygen dynamics and distribution features, e.g. burrow oxygen dynamics were linked to the lumen oxygen pattern (Fig. 9b), and the oxygen concentration was lower but the oxygen fluctuation higher in the burrow lumen in the deeper zone, Z2 (Z1: 70.7 ± 8.8 µmol l^{-1}; Z2: 44.2 ± 13.6

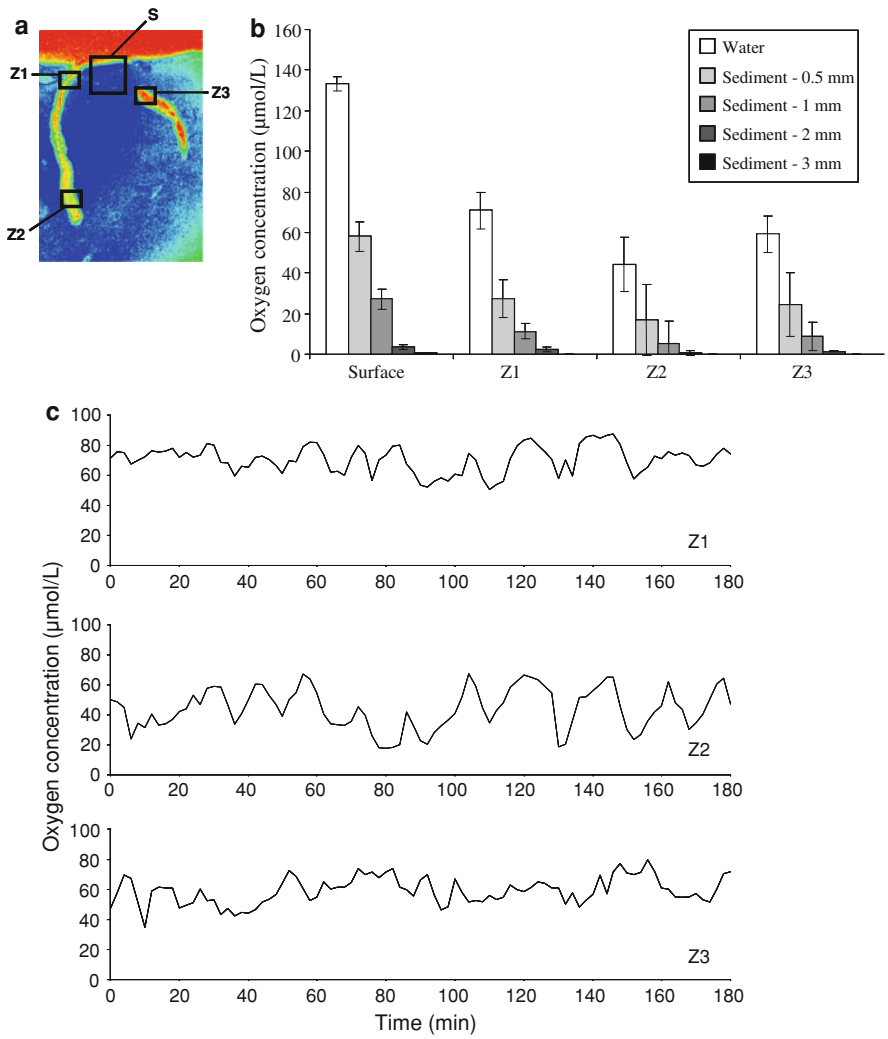

Fig. 9 (Colour online) **a** Optode image (*grey* scale images were converted to false colour) of oxygen distribution in sediments and in the *H. diversicolor* burrow and location of the zones investigated (Burrow zones: Z1–Z3; surface: S); **b** mean oxygen concentrations in free water and sediments (0.5–3 mm distance from the interface) in the overlying water and the *H. diversicolor* burrow (OW and zones Z1–Z3, respectively). *Error bars* represent the standard deviation (SD) for $N = 121$; **c** dynamics of oxygen concentration in the *H. diversicolor* burrow lumen (zones Z1–Z3)

μmol l^{-1}; Z3: 59.2 ± 8.9 μmol l^{-1}; mean ± SD, $N = 455$; Fig. 9c). This allows us to consider that the features demonstrated in the studied burrow can be extrapolated to burrows in general.

Also, in order to be able to assess the representativeness of the *H. diversicolor* burrow we studied, we have to consider how its characteristics could in fact vary. The oxygen-related functioning of a burrow can be modified by:

- the bio-irrigation pattern of *H. diversicolor* that can change depending on the worm feeding strategy—deposit-feeding, filter-feeding, herbivore or carnivore (Esnault et al., 1990; Riisgard, 1991)—which is linked to food availability and quality, the presence or absence of predators, the tidal height and season (Esselink & Zwarts, 1989; Masson et al., 1995), and the water temperature (Gerino, 1989);
- the age of the burrow, which could potentially modify the local hydrodynamics due to the increased complexity of galleries' system (Davey, 1994) and also affect the bacterial structure within the burrow (Marinelli et al., 2002).

Such differences in oxygen supply, in burrow microstructure and in the microbial communities living within the burrow microenvironment would modify the oxygen content and the diffusive properties of the burrow wall. An in situ study by Wenzhöfer & Glud (2004) in a shallow environment dominated by *H. diversicolor* also documented a highly dynamic distribution of oxygen in the burrow wall, which varied with time on a diel scale and with the environmental conditions. Thus, the data obtained in this study can be considered to be representative of what can happen to oxygen fluxes and distribution, under the specific conditions in the burrow of a specimen of this species.

Conclusion

This study shows that oxygen is heterogeneously distributed in the lumen and wall of an *H. diversicolor* burrow. More specifically, the properties (size and duration of oxygenation) of the three micro-horizons surrounding the burrow lumen (oxic, oscillating and anoxic) are spatially and temporally variable within the structure. The distribution of oxygen within the burrow seems to be controlled by (i) the distance from the sediment–water interface and (ii) the direction of water circulation resulting from active ventilation. Moreover, in the upper part of the structure, a 'buffer effect', induced by the proximity of the overlying water, reduces the variations in oxygen levels in the burrow lumen and wall. These findings about the depth-dependence and temporal variation of oxygen concentration add substantially to our understanding of *H. diversicolor* burrow function. In doing so, it goes some way towards meeting the requirement formulated by Koretsky et al. (2002) for the development of ecology-based bio-irrigation models necessary to estimate the ecological importance of burrowing species in coastal ecosystems.

Acknowledgments This study is part of Laura Pischedda's PhD research. The study was supported by the EU Commission (STREP COBO; contract number GOCE-CT-2003-505564) and the French programme ANR DHYVA (project ANR-06-SEST-09). We thank Dr. David Nerini and Dr. Matthias Gauduchon for constructive discussions and advice on the statistics and the flux calculation. Thanks are also due to the anonymous reviewers for thoughtful comments which improved the original manuscript. Nereis Park contribution number 28.

References

Aller, R. C., 1980. Quantifying solute distribution in the bioturbated zone of marine sediments by defining an average microenvironment. Geochimica et Cosmochimica Acta 44: 1955–1965.

Aller, R. C., 1988. Benthic fauna and biogeochemical processes in marine sediments: the role of burrow structures. In Blackburn, T. H. & J. Sorensen (eds), Nitrogen Cycling in Coastal Marine Environments. Wiley, Chichester: 301–338.

Aller, R. C., 1994. Bioturbation and remineralization of sedimentary organic matter: effects of redox oscillation. Chemical Geology 114: 331–345.

Aller, R. C., 2001. Transport and reactions in the bioirrigated zone. In Boudreau, B. P. & B. B. Jørgensen (eds), The Benthic Boundary Layer: Transport processes and Biogeochemistry. Oxford Press, Oxford: 269–301.

Aller, J. Y. & R. C. Aller, 1986. Evidence for localized enhancement of biological activity associated with tube and burrow structures in deep sea sediments at the Hebble site, Western North-Atlantic. Deep-Sea Research Part A–Oceanography Research Papers 33: 755–790.

Aller, R. C., J. Y. Yingst & W. J. Ullman, 1983. Comparative biogeochemistry of water in intertidal *Onuphis* (polychaeta) and *Upogebia* (crustacean) burrows—temporal pattern and causes. Journal of Marine Research 41(3): 571–604.

Anderson, J. G. & P. S. Meadows, 1978. Microenvironments in marine sediments. Proceeding of the Royal Society of Edinburgh, Section B 76: 1–16.

Bartels-Hardege, H. D. & E. Zeeck, 1990. Reproductive behavior of Nereis *diversicolor* (Annelida, Polychaeta). Marine Biology 106(3): 409–412.

Behrens, J. W., H. J. Stahl, J. F. Steffensen & R. N. Glud, 2007. Oxygen dynamics around buried lesser sandeels *Ammodytes tobianus* (Linnaeus 1785): mode of ventilation and oxygen requirements. Journal of Experimental Biology 210: 1006–1014.

Berner, R. A., 1980. Early Diagenesis: A Theorical Approach. Princeton University Press, Princeton, NJ

Bertics, V. J. & W. Ziebis, 2010. Bioturbation and the role of microniches for sulfate reduction in coastal marine sediments. Environmental Microbiology 12: 3022–3034.

Bertics, V. J., J. A. Sohm, T. Treude, C. E. Chow, D. G. Capone, J. A. Fuhrman & W. Ziebis, 2010. Burrowing deeper into benthic nitrogen cycling: the impact of bioturbation on nitrogen fixation coupled to sulfate reduction. Marine Ecology Progress Series 409: 1–15.

Boudreau, B. P., 1996. The diffusive tortuosity of fine-grained unlithified sediments. Geochimica et Cosmochimica Acta 60(16): 3139–3142.

Boudreau, B. P. & R. L. Marinelli, 1994. A modeling study of discontinuous biological irrigation. Journal of Marine Research 52: 947–968.

Caradec, S., V. Grossi, F. Gilbert, C. Guigue & M. Goutx, 2004. Influence of various redox conditions on the degradation of microalgal triacylglycerols and fatty acids in marine sediments. Organic Geochemistry 35: 277–287.

Davey, J. T., 1994. The architecture of the burrow of *Nereis diversicolor* and its quantification in relation to sediment-water exchange. Journal of Experimental Marine Biology and Ecology 179: 115–129.

Defretin, B., 1971. The tubes of polychaete annelids. In Florkin, M. & E. H. Stotz (eds), Comprehensive Biochemistry. Elsevier, Amsterdam: 713–747.

Dunn, R. J. K., D. T. Welsh, M. A. Jordan, P. R. Teasdale & C. J. Lemckert, 2009. Influence of natural amphipod (*Victoriopisa australiensis*) (Chilton, 1923) population densities on benthic metabolism, nutrient fluxes, denitrification and DNRA in sub-tropical estuarine sediment. Hydrobiologia 628: 95–109.

Duport, E., G. Stora, P. Tremblay & F. Gilbert, 2006. Effects of population density on the sediment mixing induced by the gallery-diffusor *Hediste (Nereis) diversicolor* O.F. Müller, 1776. Journal of Experimental Marine Biology and Ecology 336: 33–41.

Esnault, G., C. Retière & R. Lambert, 1990. Food resource partitioning in a population of *Nereis diversicolor* (Annelida, Polychaeta) under experimental conditions. In Proceedings of the 24th European Marine Biology Symposium: 453–467.

Esselink, P. & L. Zwarts, 1989. Seasonal trend in burrow depth and tidal variation in feeding-activity of *Nereis Diversicolor*. Marine Ecology Progress Series 56(3): 243–254.

Fenchel, T., 1996. Worm burrows and oxic microniches in marine sediments. 1. Spatial and temporal scales. Marine Biology 127: 289–295.

Forster, S. & G. Graf, 1995. Impact of irrigation on oxygen flux into the sediment—intermittent pumping by *Callianassa subterranea* and piston pumping by *Lanice conchilega*. Marine Biology 123: 335–346.

Foster-Smith, R. L., 1978. An analysis of water flow in tube-living animals. Journal of Experimental Marine Biology and Ecology 341: 73–95.

François, F., M. Gerino, G. Stora, J. Durbec & J. C. Poggiale, 2002. Functional approach to sediment reworking by gallery-forming macrobenthic organisms: modeling and application with the polychaete *Nereis diversicolor*. Marine Ecology Progress Series 229: 127–136.

Furukawa, Y., 2001. Biogeochemical consequences of macrofauna burrow ventilation. Geochemical Transactions 2(1): 83.

Gerino, M., 1989. Approche des processus de bioturbation : une technique de mesure de la bio-irrigation. Journal de la Recherche Océanographique 1–2: 24–27.

Gilbert, F., S. Hulth, V. Grossi, J. C. Poggiale, G. Desrosiers, R. Rosenberg, M. Gerino, F. Francois-Carcaillet, E. Michaud & G. Stora, 2007. Sediment reworking by marine benthic species from the Gullmar Fjord (Western Sweden): importance of faunal biovolume. Journal of Experimental Marine Biology and Ecology 348: 133–144.

Gillet, P., 1993. Impact de l'implantation d'un barrage sur la dynamique des populations de *Nereis diversicolor* (Annélide polychète) de l'estuaire du Bou Regreg, Maroc. Journal de la Recherche Océanographique 18: 15–18.

Glud, R. N., N. B. Ramsing, J. K. Gundersen & I. Klimant, 1996. Planar optrodes: a new tool for fine scale measurements of two-dimensional O_2 distribution in benthic communities. Marine Ecology Progress Series 140: 217–226.

Glud, R. N., J. K. Gundersen, H. Roy & B. B. Jørgensen, 2003. Seasonal dynamics of benthic O_2 uptake in a semi-enclosed bay: importance of diffusion and faunal activity. Limnology and Oceanography 48: 1265–1276.

Hannides, A. K. S. M., R. C. Dunn & Aller, 2005. Diffusion of organic and inorganic solutes through macrofaunal mucus secretions and tube linings in marine sediments. Journal of Marine Research 63: 957–981.

Hansen, K. & E. Kristensen, 1998. The impact of the polychaete *Nereis diversicolor* and enrichment with macroalgal (*Chaetomorpha linum*) detritus on benthic metabolism and nutrient dynamics in organic-poor and organic-rich sediment. Journal of Experimental Marine Biology and Ecology 231: 201–223.

Hulth, S., R. C. Aller, P. Engstrom & E. Selander, 2002. A pH fluorosensor (optode) for early diagenetic studies of marine sediments. Limnology and Oceanography 47(1): 212–220.

Jahn, A., R. Oeschger & H. Theede, 1992. Effects of hydrogen sulfide on the metabolism of selected polychaetes from the North Sea and the Baltic. Verhandlungen der Deutschen Zoologischen Gesellschaft 85(1): 22 (in German).

Jørgensen, B. B., 1983. Processes at the sediment-water interface. In Bolin, B. & R. B. Cook (eds), The Major Biogeochemical Cycles and Their Interactions. Scope 21, Stockholm: 477–509.

Jørgensen, B. B. & N. P. Revsbech, 1985. Diffusive boundary layers and the oxygen uptake of sediments and detritus. Limnology and Oceanography 30: 111–122.

Kautsky, H., 1939. Quenching of luminescence by oxygen. Transactions of the Faraday Society 35: 216–219.

Klimant, I., V. Meyer & M. Kuhl, 1995. Fiber-optic oxygen microsensors, a new tool in aquatic biology. Limnology and Oceanography 40: 1159–1165.

Koretsky, C. M., C. Meile & P. Van Cappellen, 2002. Quantifying bioirrigation using ecological parameters: a stochastic approach. Geochemical Transactions 3(3): 17–33.

Kristensen, E., 1981. Direct measurement of ventilation and oxygen uptake in 3 species of tubicolous polychaetes (*Nereis* spp.). Journal of Comparative Physiology B 145: 45–50.

Kristensen, E., 1983. Ventilation and oxygen uptake by three species of Nereis (Annelida, Polychaeta).1. Effects of hypoxia. Marine Ecology Progress Series 12: 289–297.

Kristensen, E., 1985. Oxygen and inorganic nitrogen exchange in a *Nereis virens* (Polychaeta) bioturbated sediment water system. Journal of Coastal Research 1: 109–116.

Kristensen, E., 1989. Oxygen and carbon-dioxide exchange in the Polychaete *Nereis virens*—influence of ventilation activity and starvation. Marine Biology 101(3): 381–388.

Kristensen, E., 2000. Organic matter diagenesis at the oxic/anoxic interface in coastal marine sediments, with emphasis on the role of burrowing animals. Hydrobiologia 426(1–3): 1–24.

Kristensen, E., 2001. Impact of polychaetes (*Nereis* and *Arenicola*) on sediment biogeochemistry in coastal areas: past, present, and future developments. Abstracts of Papers of the American Chemical Society 221: U538.

Kristensen, E. & K. Hansen, 1999. Transport of carbon dioxide and ammonium in bioturbated (*Nereis diversicolor*) coastal, marine sediments. Biogeochemistry 45(2): 147–168.

Kristensen, E., M. H. Jensen & R. C. Aller, 1991. Direct measurement of dissolved inorganic nitrogen exchange and denitrification in individual polychaete (*Nereis virens*) burrows. Journal of Marine Research 49(2): 355–377.

Liebsch, G., L. Klimant, B. Frank, G. Holst & O. S. Wolfbeis, 2000. Luminescence lifetime imaging of oxygen, pH, and carbon dioxide distribution using optical sensors. Applied Spectroscopy 54: 548–559.

Marinelli, R. L., C. R. Lovell, S. G. Wakeham, D. B. Ringelberg & D. C. White, 2002. Experimental investigation of the control of bacterial community composition in macrofaunal burrows. Marine Ecology Progress Series 235: 1–13.

Masson, S., G. Desrosiers & C. Retiere, 1995. Périodicité d'alimentation du polychète *Nereis virens* (OF Müller) selon les changements de la Marée. Écoscience 2: 20–27.

Meile, C. & P. Van Cappellen, 2003. Global estimates of enhanced solute transport in marine sediments. Limnology and Oceanography 48: 777–786.

Mettam, C., 1979. Seasonal changes in populations of *Nereis diversicolor* OF Müller from the Severn estuary UK. In Nelor, E. & R. G. Hartnoll (eds), Cyclic Phenomena in Marine Plants and Animals. Pergamon Press, Oxford: 123–130.

Meysman, F. J. R., O. S. Galaktionov, B. Gribsholt & J. J. Middelburg, 2006. Bio-irrigation in permeable sediments: an assessment of model complexity. Journal of Marine Research 64(4): 589–627.

Miron, G. & E. Kristensen, 1993. Behavioral response of three nereid polychaetes to injection of sulfide inside burrows. Marine Ecology Progress Series 101(1–2): 147–155.

Osovitz, C. J. & D. Julian, 2002. Burrow irrigation behavior of *Urechis caupo*, a filter-feeding marine invertebrate, in its natural habitat. Marine Ecology Progress Series 245: 149–155.

Pagès, A., P. R. Teasdale, D. Robertson, W. W. Bennett, J. Schäfer & D. T. Welsh, 2011. Representative measurement of two-dimensional reactive phosphate distributions and co-distributed iron(II) and sulfide in seagrass sediment porewaters. Chemosphere, in press.

Papaspyrou, S., T. Gregersen, R. P. Cox, M. Thessalou-Legaki & E. Kristensen, 2005. Sediment properties and bacterial community in burrows of the ghost shrimp *Pestarella tyrrhena* (Decapoda: Thalassinidea). Aquatic Microbial Ecology 38: 181–190.

Papaspyrou, S., T. Gregersen, E. Kristensen, B. Christensen & R. P. Cox, 2006. Microbial reaction rates and bacterial communities in sediment surrounding burrows of two nereid polychaetes (*Nereis diversicolor* and *N. virens*). Marine Biology 148: 541–550.

Papaspyrou, S., E. Kristensen & M. Thessalou-Legaki, 2010. Degradation of refractory organic matter in sandy sediment as a function of infaunal (*Nereis diversicolor*) abundance. Journal of Experimental Marine Biology and Ecology 393: 148–157.

Papkovsky, D. B., J. Olah, I. V. Troyanovsky, N. A. Sadovsky, V. D. Rumyantseva, A. F. Mironov, A. I. Yaropolov & A. P. Savitsky, 1992. Phosphorescent polymer films for optical oxygen sensors. Biosensors & Bioelectronics 7: 199–206.

Pischedda, L., J. C. Poggiale, P. Cuny & F. Gilbert, 2008. Imaging oxygen distribution in marine sediments. The importance of bioturbation and sediment heterogeneity. Acta Biotheoretica 56: 123–135.

Polerecky, L., N. Volkenborn & P. Stief, 2006. High temporal resolution oxygen imaging in bioirrigated sediments. Environmental Science and Technology 40(18): 5763–5769.

Rasmussen, H. & B. Jørgensen, 1992. Microelectrode studies of seasonal oxygen uptake in a coastal sediment: role of molecular diffusion. Marine Ecology Progress Series 81: 289–303.

Reise, K., 2002. Sediment mediated species interactions in coastal waters. Journal of Sea Research 48: 127–141.

Richter, R., 1952. Fluidal texture in sediment Gesteinen und über sedifluktion überhaupt. Notizblatt des Hessisches Landesamt für Bodenfor-schung Wiesbaden 3: 67–81.

Riisgard, H. U., 1991. Suspension feeding in the Polychaete *Nereis Diversicolor*. Marine Ecology Progress Series 70(1): 29–37.

Riisgard, H. U. & P. S. Larsen, 2005. Water pumping and analysis of flow in burrowing zoobenthos: an overview. Aquatic Ecology 39: 237–258.

Robertson, D., D. T. Welsh & P. R. Teasdale, 2009. Investigating biogenic heterogeneity in coastal sediments with two-dimensional measurements of iron(II) and sulfide. Environmental Chemistry 6: 60–69.

Rosenberg, R., 2001. Marine benthic faunal successional stages and related sedimentary activity. Scientia Marina 65: 107–119.

Scaps, P., 2002. A review of the biology, ecology and potential use of the common ragworm *Hediste diversicolor* (OF Muller) (Annelida: Polychaeta). Hydrobiologia 470(1–3): 203–218.

Schottler, U., 1979. On the anaerobic metabolism of three species of Nereis (Annelida). Marine Ecology Progress Series 1: 249-254.

Strömberg, N., 2006. Imaging Optodes. PhD thesis, University of Göteborg, Göteborg.

Stromberg, N. & S. Hulth, 2003. A fluorescence ratiometric detection scheme for ammonium ions based on the solvent sensitive dye MC 540. Sensors and Actuators B: Chemical 90(1–3): 308–318.

Sun, M. Y., R. C. Aller, C. Lee & S. G. Wakeham, 2002. Effects of oxygen and redox oscillation on degradation of cell-associated lipids in surficial marine sediments. Geochimimica et Cosmochimica Acta 66: 2003–2012.

Timmermann, K., G. T. Banta & R. N. Glud, 2006. Linking *Arenicola marina* irrigation behavior to oxygen transport and dynamics in sandy sediments. Journal of Marine Research 64: 915–938.

Vedel, A. & H. U. Riisgard, 1993. Filter-feeding in the polychaete *Nereis diversicolor*: growth and bioenergetics. Marine Ecology Progress Series 100: 145–152.

Vismann, B., 1990. Sulfide detoxification and tolerance in *Nereis* (*Hediste*) *diversicolor* and *Nereis* (*Neanthes*) *virens* (Annelida: Polychaeta). Marine Ecology Progress Series 59: 229–238.

Wenzhöfer, F. & R. N. Glud, 2004. Small-scale spatial and temporal variability in coastal benthic O_2 dynamics: effects of fauna activity. Limnology and Oceanography 49(5): 1471–1481.

Zhu, Q., R. C. Aller & F. Yanzhen, 2006. A new ratiometric, planar fluorosensor for measuring high resolution, two-dimensional pCO_2 distributions in marine sediments. Marine Chemistry 101(1–2)(40): 40–53.